DECREASING THE MEASUREMENT TIME OF BLOOD SUGAR TESTS USING PARTICLE FILTERING

Ann-Kathrin Seifert, Nevine Demitri, Abdelhak M. Zoubir

Signal Processing Group, Institute of Telecommunications
Technische Universität Darmstadt, Merckstr. 25, 64283
Darmstadt, Germany
{seifert, demitri, zoubir}@spg.tu-darmstadt.de

ABSTRACT

The usability of hand-held glucose meters to self-monitor blood sugar levels is crucially affected by the measurement time. We consider an image-based photometric measurement setup that optically tracks the chemical reaction that takes place on the blood covered test strip. The aim is to obtain a reliable estimate of the true underlying glucose concentration in the blood sample at an early stage of the observed chemical reaction in order to increase the testing speed. We propose using particle filtering to track the required image statistics that are subject to a non-linear process. Using real data, we show that the developed algorithm drastically reduces the measurement time at a comparable quality of results.

***Index Terms*—** Particle filter, Bayes filter, glucose measurement, measurement time, usability

1. INTRODUCTION

According to the World Health Organization (WHO) more than 347 million people worldwide currently suffer from diabetes [1]. Frequent self-monitoring of blood sugar levels using small hand-held devices, so-called glucose meters, is essential for diabetics in order to obviate long-term health complications such as heart disorders, kidney failures or damage of blood vessels and nerves [2].

We consider hand-held glucose meters that operate on the novel photometric measurement principle [3, 4, 5], which works with a much smaller blood sample volume compared to state-of-the-art devices [6]. Here, a camera optically tracks the chemical reaction between the blood glucose and the chemical agent on the test strip, which leads to a color change of the test strip. In order to estimate the underlying glucose concentration, we require the intensity value of the region of interest (ROI), i.e. the part of the test strip that reveals the chemical reaction.

Ideally, we are interested in the intensity value of the ROI at the saturation stage of the chemical reaction, which is identified by a constant color of the ROI. However, waiting for the chemical reaction to reach this stage conflicts with the aim of a fast measurement. A decreased measurement time is of special interest in order to reduce inconvenience to the patient. Hence, the usability of hand-held glucose meters is crucially affected by the measurement time.

We propose a state-space approach to obtain an estimate of the underlying glucose concentration at an early stage of the monitored chemical reaction such that the measurement time is decreased. Being able to model the temporal evolution of the observed chemical reaction, we apply particle filtering for online prediction of the required image statistics. Particle filters have become a popular tool for various visual tracking applications, see e.g. [7]. They are capable of dealing with non-linear state-space models and are suitable for tracking multi-modal distributions [8, 9], which are both needed to solve the state estimation problem at hand. In fact, particle filtering has also been applied for glucose measurements, as e.g. in [10], to predict the daily progress of a patient's blood glucose level so as to ensure optimal treatment. However, to the best of our knowledge, so far there is no previous work on decreasing the measurement time of glucose measurements using a photometric measurement setup.

2. IMAGE-BASED PHOTOMETRIC MEASUREMENT PRINCIPLE

The photometric measurement principle is commonly used to determine the concentration of an analyte in a fluid [5], such as glucose in a blood sample [4, 3]. First, a blood sample is placed on a test strip, which carries a chemical agent. Then, the blood glucose reacts with the chemical agent yielding a color change of the test strip. A light-emitting diode (LED) illuminates the test strip, such that the color change can be tracked optically by a camera. The captured images are preprocessed [6] and the ROI is determined by applying a statistical image segmentation method using, e.g., a clustering approach [11]. For each image, we measure the amount of light reflected from the ROI, referred to as relative remission R_{ROI}. At the saturation stage of the chemical reaction, we observe R_{sat}, which can be directly mapped to the underlying

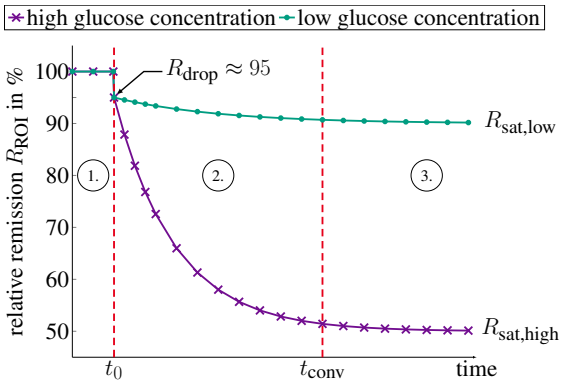

Fig. 1. Idealized model of the temporal behavior of the chemical reaction for high and low glucose concentrations.

glucose concentration C in the blood sample. The saturation stage is identified by tracking the temporal development of R_{ROI} and is characterized by a constant intensity level.

The temporal evolution of R_{ROI} yields the kinetic curve, which characteristizes the observed chemical reaction. Fig. 1 shows two idealized kinetic curves for a low and a high glucose concentration. Typically, the kinetic curve reveals three stages of the chemical reaction [12]:

1. Constant intensity stage for $t < t_0$: the chemical reaction has not started yet.
2. Moistening period for $t \geq t_0$: the blood sample is recognized by the chemical agent and the reaction starts; after a rapid drop in relative remission to R_{drop}, the kinetic curve decays exponentially.
3. Convergence at $t = t_{\text{conv}}$: at the saturation stage of the chemical reaction, the kinetic curve approaches the final relative remission value R_{sat}.

Fig. 2 shows examples of measurement images and corresponding histograms of image intensities at different times of the chemical reaction. Typically, the histograms reveal two major modes, which can be associated with the ROI and the remainder of the test strip, respectively. In the beginning, the two modes lie closely together. As the chemical reaction proceeds, the ROI mode moves towards lower intensity levels. For high glucose concentrations, the two modes become clearly separated at the convergence stage. Here, the color change is more prominent than for low glucose concentrations, for which the two modes remain closely together.

In contrast to the previously described state-of-the-art method, we claim that modeling the temporal evolution of the probability density function (PDF) of relative remission values is useful to obtain a reliable estimate of the underlying glucose concentration already at an early stage of the observed chemical reaction. In particular, we can predict image statistics, e.g. the histogram modes at the saturation stage by using a Bayesian approach and online particle filtering, as explained in the following section.

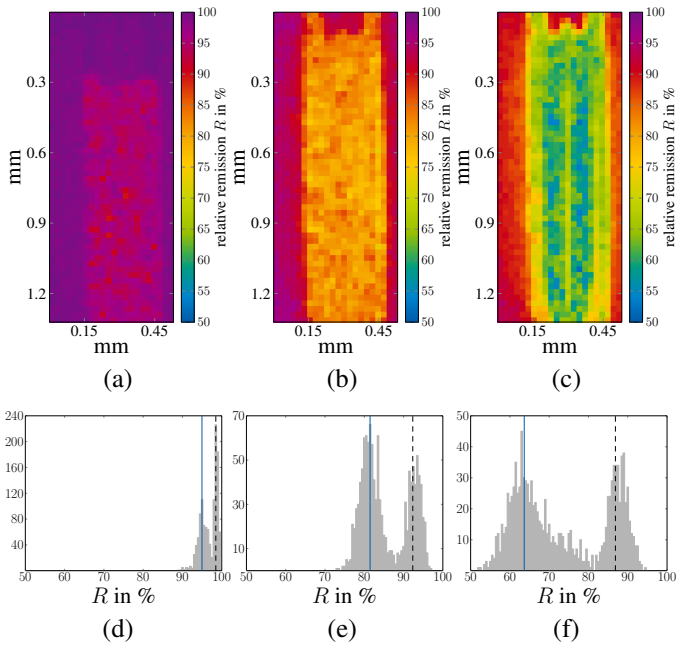

Fig. 2. Examples of measurement images and the corresponding histograms with modes. (a)+(d) At $t = t_0$ the chemical reaction has just started and the modes lie closely together. (b)+(e) For $t > t_0$ the ROI mode moves towards lower intensity values, until (c)+(f) the modes are fully separated at convergence for $t = t_{\text{conv}}$. In Fig. (d)-(f) the y-axis indicates the absolute frequency of occurrence of relative remission values.

3. BAYESIAN APPROACH AND PARTICLE FILTERING

The recursive Bayesian filtering approach is commonly used to solve dynamic state estimation problems [13, 8, 14]. Using a Markovian probabilistic model for the state evolution, the complete solution to the stochastic filtering problem can be expressed in a recursive manner using the system model (prior) $p(\mathbf{x}_t|\mathbf{x}_{t-1})$ and the observation model (likelihood) $p(\mathbf{y}_t|\mathbf{x}_t)$. Given that the initial PDF $p(\mathbf{x}_0)$ is known, we can infer the state of the system $\mathbf{x}_t$ at time instant t as soon as a new observation $\mathbf{y}_t$ becomes available. Typically, we are interested in a particular marginal of the posterior PDF, the so-called *filtering distribution* $p(\mathbf{x}_t|\mathbf{y}_{1:t})$, which can be recursively estimated by making use of the Chapman-Kolmogorov equation and Bayes' rule [8] as

$$p(\mathbf{x}_t|\mathbf{y}_{1:t}) \propto p(\mathbf{y}_t|\mathbf{x}_t) \int p(\mathbf{x}_t|\mathbf{x}_{t-1})\, p(\mathbf{x}_{t-1}|\mathbf{y}_{1:t-1})\, d\mathbf{x}_{t-1}. \tag{1}$$

From the filtering distribution, we can obtain an optimal estimate of the system state, such as a minimum mean squared error (MMSE) or maximum a posteriori (MAP) estimate.

However, an analytic solution to evaluate the filtering distribution in (1) exists only in some special cases with

restrictive assumptions [15]. For many practical applications, non-linear Bayesian filters are used as they allow for less restrictive assumptions on the system models. Applying Monte Carlo (MC) sampling techniques, such as importance sampling (IS), the optimal solution may be approximated numerically. In the recursive case, IS forms the basis of the sequential importance sampling (SIS) algorithm, which is the core technique of particle filters [8, 13].

Particle filters propagate a set of N_p random samples, called *particles*, with associated scalar weights, $\{(\mathbf{x}_t^i, w_t^i)\}_{i=1}^{N_p}$, through the given system to approximate the filtering distribution $p(\mathbf{x}_t|\mathbf{y}_{1:t})$ by

$$p(\mathbf{x}_t|\mathbf{y}_{1:t}) \approx \sum_{i=1}^{N_p} w_t^i \, \delta(\mathbf{x}_t - \mathbf{x}_t^i), \tag{2}$$

where $\delta(\cdot)$ denotes Dirac's delta function and the weights are normalized such that $\sum_{i=1}^{N_p} w_t^i = 1$ [8]. Using SIS, the importance weights are recursively updated by

$$w_t^i \propto w_{t-1}^i \, \frac{p(\mathbf{y}_t|\mathbf{x}_t^i) \, p(\mathbf{x}_t^i|\mathbf{x}_{t-1}^i)}{q(\mathbf{x}_t^i|\mathbf{x}_{t-1}^i, \mathbf{y}_t)}, \tag{3}$$

where $q(\mathbf{x}_t|\mathbf{x}_{t-1}, \mathbf{y}_t)$ refers to the so-called *proposal distribution*, which covers the support of the filtering distribution $p(\mathbf{x}_t|\mathbf{y}_{1:t})$ and from which we can easily draw particles such that $\mathbf{x}_t^i \sim q(\mathbf{x}_t|\mathbf{x}_{t-1}^i, \mathbf{y}_t)$ with $i = 1, ..., N_p$ [13]. Note that for a very large number of particles, (2) is equivalent to a functional description. Thus, we obtain a weighted approximation of the MMSE estimate for the state of the system $\mathbf{x}_t$ as [13]

$$\hat{\mathbf{x}}_t^{\text{MMSE}} \approx \sum_{i=1}^{N_p} w_t^i \, \mathbf{x}_t^i. \tag{4}$$

4. PROPOSED ALGORITHM

4.1. Modeling and State-space Approach

Generally, we are interested in the final remission value of the ROI R_{sat}. In principle, this value is not accessible until the chemical reaction has saturated. However, we can model the temporal behavior of the chemical reaction for $t \geq t_0$ as [16]

$$R(t) = (R_{\text{drop}} - R_{\text{sat}}) \cdot \mathrm{e}^{\tau(t-t_0)} + R_{\text{sat}}, \tag{5}$$

where R_{drop} is the relative remission value after the drop of the kinetic curve at $t = t_0$ and τ denotes the decay rate.

Following a state-space approach, we define the static state of the system as the true final remission value R_{sat} and observations as pixel intensity values of a pre-processed image, which is described by the matrix $\mathbf{I}^{M\times N}$. Here, M and N are the number of pixels in vertical and horizontal direction, respectively. Each image element $\mathrm{I}(m, n)$ for $m = 1, ..., M$ and $n = 1, ..., N$ describes a pixel's intensity value and represents the measured relative remission at the corresponding location in the image.

4.2. System and Observation Model

We explicitly introduce a dynamic to the originally static state of the system. Thus, the state is artificially made to follow a first order Markov process, where the current state only depends on the previous state given a random walk dynamic with small variance. This application-driven solution, formally known as artificial evolution of parameters [17, 18], eases the need of perfect initialization of the particle filter and decreases the problem of sample degeneracy as potentially more particles obtain a significant weight in the update stage via (3). Hence, the system model is given by

$$R_{\text{sat},t} = R_{\text{sat},t-1} + u_{t-1}, \tag{6}$$

where u is an i.i.d. additive zero-mean Gaussian noise component distributed according to $u_t \sim \mathcal{N}(0, \sigma_u^2) \; \forall \, t \in \mathbb{R}$.

For the observation model we use (5) to relate an observation $\mathrm{I}_t(m, n)$ at time instant t to the state $R_{\text{sat},t}$ as

$$\mathrm{I}_t(m,n) = (R_{\text{drop}} - R_{\text{sat},t}) \cdot \mathrm{e}^{\tau\cdot(t-t_0)} + R_{\text{sat},t} \; \forall \, (m,n) \in M \times N. \tag{7}$$

Note that in the following we will drop the pixel location index (m, n) for national convenience when referring to a single measurement pixel.

4.3. Particle Filtering

We choose particle filters to solve the given state estimation problem as they are able to deal with the required multi-modal PDF of image intensities as well as with the non-linear observation model. Here, we design two parallel, identical particle filters that operate on different image regions, which together form the region-based particle filter (RBPF). The image regions are chosen such that one region is most likely to include the ROI, and another region that most probably does not contain ROI pixels. Overlapping regions are chosen to account for uncertainty about the exact location of the ROI in the captured images.

For the design of the RBPF we use the system model in (6) to formulate the prior as

$$p(R_{\text{sat},t}^i | R_{\text{sat},t-1}^i) = \mathcal{N}(R_{\text{sat},t}^i; R_{\text{sat},t-1}^i, \sigma_u^2), \tag{8}$$

which is used as the proposal distribution such that (3) reduces to

$$w_t^i \propto w_{t-1}^i \, p(\mathrm{I}_t | R_{\text{sat},t}^i). \tag{9}$$

The likelihood $p(\mathrm{I}_t|R_{\text{sat},t}^i)$ is found by evaluating a kernel density estimate $\hat{f}$ of the PDF of observed pixel intensities $\mathcal{I}_t = \{\mathrm{I}_t^j\}_{j=1}^{M\times N}$ at I_t, which is obtained using (7), such that

$$p(\mathrm{I}_t | R_{\text{sat},t}^i) = \hat{f}(\mathrm{I}_t; \mathcal{I}_t, h), \tag{10}$$

where we use a kernel density estimator based on a Gaussian kernel function with adaptive bandwidth parameter h.

	Ref	RBPF
$C \leq 100$	0.37	1.06
$C > 100$	0.01	0.02
Overall	**0.10**	**0.28**

(a) Variation coefficient.

	Ref	RBPF
$C \leq 75$	11.41	7.56
$C > 75$	8.03	11.55
Overall	**8.64**	**10.83**

(b) gMAD in mg/dl.

Table 1. Comparison of glucose-specific evaluation methods for the reference (Ref) and the proposed algorithm (RBPF) for different underlying glucose concentrations C in mg/dl.

We note that the RBPF generally enables the use of two different likelihood formulations: one for the ROI and one for the remainder of the test strip. However, we found that (7) models the temporal evolution of non-ROI pixels sufficiently well. In order to mitigate *sample degeneracy*, i.e. all but a few samples will have negligible weight after a few iterations, the particles are resampled at each time step [8].

5. EXPERIMENTAL RESULTS

5.1. Data Set and Setup

The available data set consists of 78 measurement videos that were obtained using the setup as described in Sec. 2. The measurements were taken using whole blood samples with 16 different underlying glucose concentrations ranging from 30 mg/dl to 550 mg/dl. Each video is of 20 s duration and the camera takes 30 frames per second, such that each measurement consists of 600 frames in total. Thereof, we only consider those images that reveal the chemical reaction for $t \geq t_0$. The particle filter uses 500 particles per region and time step. Each region-based filter is initialized by a Gaussian distribution with small variance centered at 100 and R_{drop}, respectively, which approximate well the distributions of image intensities at $t = t_0$. Here, R_{drop} is obtained from the first image by utilizing the state-of-the-art method. The variance of the system noise component is chosen as $\sigma_u^2 = 3$ to overcome the straightforward initialization but to avoid sample degeneracy. The decay rate τ in (7) depends on the underlying glucose concentration and can be approximated by $\tau \approx a \cdot R_{\text{sat}} + b$. Using the available data set, the parameters are estimated as $a = -1.24 \cdot 10^{-4}$ and $b = -0.02$ via a robust non-linear least squares method. The RBPF converges as soon as the changes in both state estimates are sufficiently small. In this way the measurement time is determined.

5.2. Results

Using the RBPF for image-based photometric glucose measurement, the average testing time is reduced by approximately 50% at a comparable accuracy and precision of results as for the state-of-the-art method described in Sec. 2. Fig. 3 reveals the average measurement times for different underlying glucose concentrations. On average, the RBPF predicts

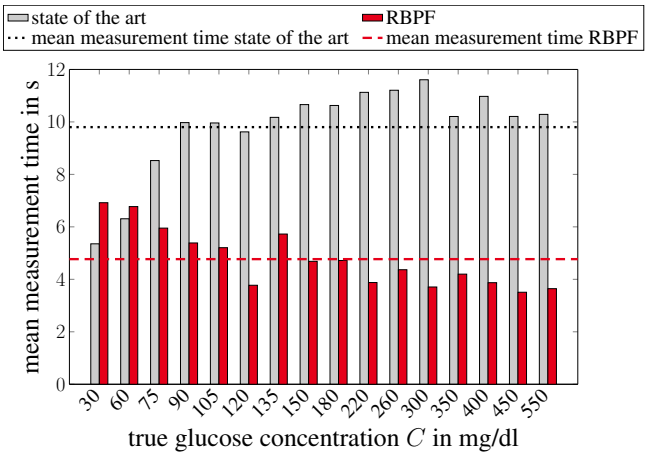

Fig. 3. Average measurement times when using the RBPF compared to the state-of-the-art method.

the required image statistics by 4.8 s compared to 9.8 s for the reference. For specific measurement groups the testing speed is even increased by 65%.

The quality of glucose measurements is assessed by appropriate evaluation methods: an inter-group variance, i.e. variation coefficient [6], that describes the precision of results and a glucose-specific mean absolute deviation (gMAD) [19], which specifies the accuracy of the measurements. The corresponding averaged values, which should both be small, are given in Table 1. We find that the overall quality of results is comparable to the reference method, as both quality measures do not deviate significantly from the reference. In fact, Table 1(b) shows that for low glucose concentrations, the RBPF leads to clinically more accurate results compared to the reference. This is an important case, as in these cases hypoglycemia is present and overestimation of the glucose concentration can be fatal to the patient.

Additionally, our MATLAB simulations reveal that on average the proposed algorithm requires less than a third of the computational complexity of the reference. This is mainly due to the fact that we can omit typically computationally costly segmentation procedures here. As a result the proposed algorithm is suitable for hand-held devices with limited power supply and storage capacities.

6. CONCLUSION AND FUTURE WORK

We have shown that applying particle filtering to the problem of image-based photometric glucose measurement in hand-held devices can drastically reduce the average testing time at a comparable quality of results. Our findings encourage to dedicate future work to tracking the complete multi-modal image PDF instead of region-based components of it. Here, a non-parametric mixture approach as outlined by Vermaak et al. in [20] or a parametric approach using ideas by Kotecha and Djurić in [21, 22] may be of interest.

7. REFERENCES

[1] W. H. Organization, "Diabetes Fact Sheet N°312," January 2015, (Retrieved: April 2015).

[2] American Diabetes Association, "Diagnosis and Classification of Diabetes Mellitus," *Diabetes Care*, vol. 37, no. 1, pp. 81–89, 2013.

[3] W. Petrich, H.-P. Haar, J.-M. Asfour, and G. Kocherscheidt, "Analyse optischer Daten mit Hilfe von Histogrammen," European Patent Application, 2007, EP 1 843 148 A1.

[4] K. Miltner, U. Ruppender, C. Wersig, and V. Zimmer, "Method for the Photometric Anaylsis of Test Elements," United States Patent, 2004, US 6,707,554 B1.

[5] F. Wehowski, B. Rosicke, and S. Kalveram, "System and Method for Acquiring and Evaluating Optical Signals," United States Patent, 2009, US 7,630,084 B2.

[6] N. Demitri and A. M. Zoubir, "Mean-shift Based Algorithm for the Measurement of Blood Glucose in Handheld Devices," *Proceedings of the 21st European Signal Processing Conference (EUSIPCO)*, pp. 1–5, 2013.

[7] P. Torr, A. Blake, R. Cipolla, A. Criminisi, A. Dick, C. Rother, B. Stenger, J. Shotton, and A. Thayananthan, "Bayesian Methods in Graphics," *International Conference Graphicon*, 2003.

[8] M. S. Arulampalam, S. Maskell, N. Gordon, and T. Clapp, "A Tutorial on Particle Filters for Online nonlinear/non-Gaussian Bayesian Tracking," *IEEE Transactions on Signal Processing*, vol. 50, no. 2, pp. 174–188, 2002.

[9] J. Candy, "Bootstrap Particle Filtering," *IEEE Signal Processing Magazine*, vol. 24, no. 4, pp. 73–85, July 2007.

[10] T. Briegel and V. Tresp, "A Nonlinear State Space Model for the Blood Glucose Metabolism of a Diabetic," *at-Automatisierungstechnik Methoden und Anwendungen der Steuerungs-, Regelungs-und Informationstechnik*, vol. 50, no. 5/2002, pp. 228, 2002.

[11] Y. A. Sheikh, E. A. Khan, and T. Kanade, "Mode-seeking by Medoidshifts," *IEEE 11th International Conference on Computer Vision (ICCV)*, pp. 1–8, 2007.

[12] N. Demitri and A. M. Zoubir, "Detection of Faulty Glucose Measurements Using Texture Analysis," *Proceedings of the 22nd European Signal Processing Conference (EUSIPCO)*, pp. 2480–2484, 2014.

[13] Z. Chen, "Bayesian Filtering: From Kalman Filters to Particle Filters, and Beyond," *Statistics*, vol. 182, no. 1, pp. 1–69, 2003.

[14] A. Doucet, S. Godsill, and C. Andrieu, "On Sequential Monte Carlo Sampling Methods for Bayesian Filtering," *Statistics and Computing*, vol. 10, no. 3, pp. 197–208, 2000.

[15] A. Doucet, N. d. Freitas, and N. Gordon, *Sequential Monte Carlo Methods in Practice*, Springer, 2001.

[16] S. Leier, "Methods of Signal Detection and Processing in Medical Engineering," Master thesis, Technische Universität Darmstadt, May 2009.

[17] J. Liu and M. West, "Combined Parameter and State Estimation in Simulation-based Filtering," in *"Sequential Monte Carlo Methods in Practice"*, pp. 197–223. Springer, 2001.

[18] N. Gordon, D. Salmond, and A. Smith, "Novel Approach to Nonlinear/Non-Gaussian Bayesian State Estimation," *IEE Proceedings F Radar and Signal Processing*, vol. 140, no. 2, pp. 107–113, Apr 1993.

[19] S. Del Favero, A. Facchinetti, and C. Cobelli, "A Glucose-Specific Metric to Assess Predictors and Identify Models," *IEEE Transactions on Biomedical Engineering*, vol. 59, no. 5, pp. 1281–1290, May 2012.

[20] J. Vermaak, A. Doucet, and P. Pérez, "Maintaining Multi-Modality through Mixture Tracking," *Ninth IEEE International Conference on Computer Vision*, vol. 2, pp. 1110–1116, Oct 2003.

[21] J. H. Kotecha and P. Djurić, "Gaussian Particle Filtering," *IEEE Transactions on Signal Processing*, vol. 51, no. 10, pp. 2592–2601, Oct 2003.

[22] J. H. Kotecha and P. Djurić, "Gaussian Sum Particle Filtering," *IEEE Transactions on Signal Processing*, vol. 51, no. 10, pp. 2602–2612, Oct 2003.